

## Formulation and Stability of Itraconazole and Odanacatib Nanoparticles: Governing Physical Parameters

Varun Kumar,<sup>†</sup> Lei Wang,<sup>‡</sup> Mike Riebe,<sup>‡</sup> Hsien-Hsin Tung,<sup>‡</sup> and Robert K. Prud'homme<sup>\*†</sup>

Chemical Engineering Department, Princeton University, Princeton New Jersey 08544, and Merck Research Laboratory, West Point, Pennsylvania 19486

Received January 2, 2009; Revised Manuscript Received April 6, 2009; Accepted April 14, 2009

**Abstract:** The successful formulation of itraconazole and odanacatib into nanoparticle form with diameters of 145 and 350 nm, respectively, using rapid, block copolymer-directed precipitation is presented. These are the smallest stable nanoparticles that have been reported for these compounds. The difference in size of the nanoparticles for the two compounds is explained by the difference in nucleation rate and its dependence on supersaturation. The conditions for stability after formation are presented: storage at 5 °C and removal of residual processing solvent. These requirements are explained in terms of solute solubility and its dependence on both temperature and solvent concentration. The theory of Ostwald ripening provides the framework for understanding the differences in stability observed for the two compounds. The dynamics of the hydrophobic polymer block plays a major role in long-term stability as demonstrated by the behavior of nanoparticles stabilized by poloxamer vs polystyrene-*b*-polyethylene oxide polymers.

**Keywords:** Nanoparticle; nucleation; precipitation; solubility; stability; supersaturation; Ostwald ripening; itraconazole; odanacatib; poloxamer

### Introduction

The recent increase in the number of hydrophobic drug compounds under evaluation<sup>1</sup> has resulted in the development of a variety of new drug carriers and formulation techniques.<sup>2,3</sup> Solvent and antisolvent exchange through dialysis<sup>4</sup> and emulsification followed by solvent stripping<sup>5</sup> are slow thermodynamically controlled processes that often result in drug/matrix phase separation and low drug loading.<sup>6</sup> Rapid

precipitation techniques<sup>3,7–10</sup> are kinetically controlled, which result in higher drug loading<sup>3</sup> and enable the creation of complex composite nanoparticles.<sup>11</sup> The mixing of an

\* Corresponding author. Mailing address: Princeton University, Chemical Engineering, A301 E-Quad, Princeton, NJ 08544. E-mail: prudhomm@princeton.edu. Phone: (609) 258 4577. Fax: (609) 258 0211.

<sup>†</sup> Princeton University.

<sup>‡</sup> Merck Research Laboratory.

(1) Lipinski, C. Poor aqueous solubility - an industry wide problem in drug discovery. *Am. Pharm. Rev.* **2002**, 5, 82–85.

(2) Hu, J.; Johnston, K. P.; Williams, R. O. Nanoparticle Engineering Processes for Enhancing the Dissolution Rates of Poorly Water Soluble Drugs. *Drug Dev. Ind. Pharm.* **2004**, 30 (3), 233–245.

(3) Johnson, B. K.; Prud'homme, R. K. Mechanism for Rapid Self-Assembly of Block Copolymer Nanoparticles. *Phys. Rev. Lett.* **2003**, 91 (11), 118302.

(4) Allen, C.; Maysinger, D.; Eisenberg, A. Nano-engineering block copolymer aggregates for drug delivery. *Colloids Surf., B* **1999**, 16 (1–4), 3–27.

(5) Song, C. X.; Labhasetwar, V.; Murphy, H.; Qu, X.; Humphrey, W. R.; Shebuski, R. J.; Levy, R. J. Formulation and characterization of biodegradable nanoparticles for intravascular local drug delivery. *J. Controlled Release* **1997**, 43 (2–3), 197.

(6) Kumar, V.; Prud'homme, R. K. Thermodynamic Limits on Drug Loading in Nanoparticle Cores. *J. Pharm. Sci.* **2008**, 97 (11), 4904–4914.

(7) Matteucci, M. E.; Hotze, M. A.; Williams, R. O.; Johnston, K. P. Drug Nanoparticles by Antisolvent Precipitation: Mixing Energy versus Surfactant Stabilization. *Langmuir* **2006**, 22 (21), 8951–8959.

(8) Reverchon, E.; De Marco, I.; Caputo, G.; Della Porta, G. Pilot scale micronization of amoxicillin by supercritical antisolvent precipitation. *J. Supercrit. Fluids* **2003**, 26 (1), 1–7.

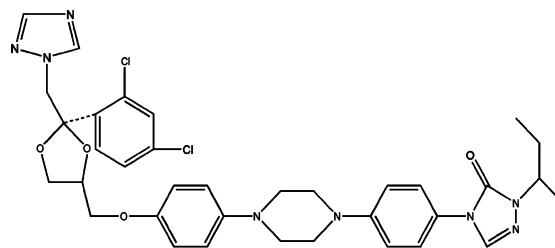
(9) Reverchon, E.; De Marco, I.; Della Porta, G. Rifampicin micro-particles production by supercritical antisolvent precipitation. *Int. J. Pharm.* **2002**, 243, 83–91.

antisolvent stream with a solvent stream containing dissolved drug and stabilizing polymers creates high supersaturation and causes the solute to rapidly nucleate and grow. The ultimate particle size is controlled by the attachment of the stabilizing copolymers to the particle surface which quenches aggregation. Different precipitation techniques have been used to formulate itraconazole (ITZ), an antifungal drug, into nanoparticle form. de Chasteigner et al.<sup>12</sup> demonstrated the use of liposome, cholesterol complexes and nanospheres as drug carriers for ITZ. The highest drug concentration achieved was 0.51 mg/mL when encapsulated in 80 nm nanospheres composed of poly caprolactone and sodium deoxycholate. However a continuous ITZ desorption from the nanospheres was observed due to poor control on the localization of ITZ molecules. Matteucci et al.<sup>7</sup> used rapid precipitation to formulate 200 nm ITZ particles. However the presence of organic solvent induced Ostwald ripening and coagulation, and as a result, particle size increased to 10  $\mu\text{m}$  in 10 min. They obtained stable ITZ particles with suitable processing of nanoparticle dispersion using salt flocculation<sup>13</sup> or lyophilization<sup>14</sup> to remove the organic cosolvent. Salt flocculation<sup>13</sup> was shown to be an efficient process for solvent removal, and particles of 290 to 680 nm could be dried and reconstituted. They formed antisolvent precipitated particles at low temperature that are stable as nanoparticles after solvent is evaporated.<sup>14</sup> These nanoparticles could be redispersed after being dried with poloxamer 407 as the stabilizer.

Odanacatib (ODA) is a hydrophobic drug compound (Figure 1) that is an inhibitor for cathepsin K, a lysosomal cysteine protease overexpressed in cells responsible for bone degradation.<sup>15,16</sup> Nanoparticle forms of ODA have not been reported in the literature.

We present the successful production of stable particles of ITZ and ODA by rapid precipitation and block copolymer stabilization. The postprocessing required to produce a stable nanoparticle dispersion is presented and discussed in terms

## ITRACONAZOLE



## ODANACATIB

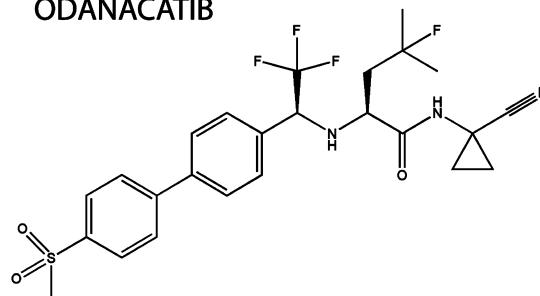


**Figure 1.** Molecular structure of itraconazole and odanacatib.<sup>14</sup>

of the mechanism of Ostwald ripening.<sup>17,18</sup> The initial formation of the nanoparticle dispersion depends on mixing, supersaturation, and nucleation and growth rates. Thereafter, stability depends on the stabilizer, solubility of the drug molecules in the solution phase, particle size, and interfacial energy. The “rules” for stable nanoparticle formulation are discussed using ITZ and ODA data as a framework for the discussion.

## Experimental Section

The experimental apparatus for particle formation is shown schematically in Figure 2 where 75 mL of water continuously circulates from the reservoir through a mixing tee (i.d. = 0.3175 cm). In the tee the organic liquid with the drug and block copolymer are introduced. At the tee, an ultrasonic probe (Branson Digital Sonifier at power setting of 40%) provides energy to aid mixing. The temperature is controlled

- (10) Young, T. J.; Mawson, S.; Johnston, K. P.; Henriksen, I. B.; Pace, G. W.; Mishra, A. K. Rapid Expansion from Supercritical to Aqueous Solution to Produce Submicron Suspensions of Water-Insoluble Drugs. *Biotechnol. Prog.* **2000**, *16* (3), 402–407.
- (11) Gindy, M. E.; Panagiotopoulos, A. Z.; Prud'homme, R. K. Composite Block Copolymer Stabilized Nanoparticles: Simultaneous Encapsulation of Organic Actives and Inorganic Nanostructures. *Langmuir* **2008**, *24* (1), 83–90.
- (12) de Chasteigner, S.; Fessi, H.; Devissaguet, J.-P.; Puisieux, F. Comparative study of the association of itraconazole with colloidal drug carriers. *Drug Dev. Res.* **1996**, *38* (2), 125–133.
- (13) Matteucci, M. E.; Paguio, J. C.; Miller, M. A.; Williams, R. O.; Johnston, K. P. Flocculated Amorphous Nanoparticles for Highly Supersaturated Solutions. *Pharm. Res.* **2008**, *25* (11), 2477–2487.
- (14) Matteucci, M. E.; Brettmann, B. K.; Rogers, T. L.; Elder, E. J.; Williams, R. O.; Johnston, K. P. Design of Potent Amorphous Drug Nanoparticles for Rapid Generation of Highly Supersaturated Media. *Mol. Pharmaceutics* **2009**, *4* (5), 782–793.
- (15) Stoch, S.; Wagner, J. Cathepsin K Inhibitors: A Novel Target for Osteoporosis Therapy. *Clin. Pharmacol. Ther.* **2008**, *83*, 172–176.

- (16) Gauthier, J. Y.; Chauret, N.; Cromlish, W.; Desmarais, S.; Duong, L. T.; Falgout, J.-P.; Kimmel, D. B.; Lamontagne, S.; Léger, S.; LeRiche, T.; Li, C. S.; Massé, F.; McKay, D. J.; Nicoll-Griffith, D. A.; Oballa, R. M.; Palmer, J. T.; Percival, M. D.; Riendeau, D.; Robichaud, J.; Rodan, G. A.; Rodan, S. B.; Seto, C.; Thérien, M.; Truong, V.-L.; Venuti, M. C.; Wesolowski, G.; Young, R. N.; Zamboni, R.; Black, W. C. The discovery of odanacatib (MK-0822), a selective inhibitor of cathepsin K. *Bioorg. Med. Chem. Lett.* **2008**, *18* (3), 923–928.
- (17) Ying, L.; Kendra, K.; Walid, S.; Prud'homme, R. K. Ostwald Ripening of beta-Carotene Nanoparticles. *Phys. Rev. Lett.* **2007**, *98* (3), 036102.
- (18) Kumar, V.; Prud'homme, R. K. Nanoparticle stability: Processing pathways for solvent removal. *Chem. Eng. Sci.* **2009**, *64* (6), 1358–1361.

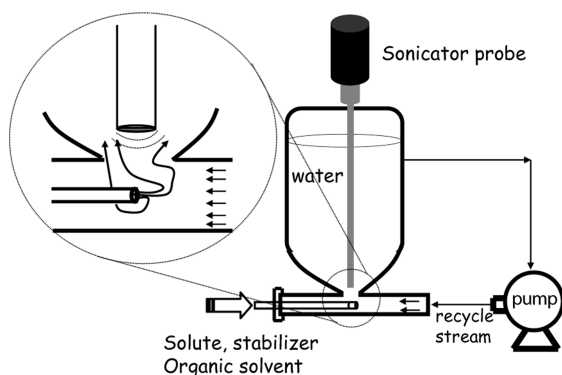


**Figure 2.** Schematic of the particle formation device. Continuous circulation of the aqueous phase is used to mix the incoming organic solvent stream with the solute and polymer stabilizer. The sonicator probe provides additional mixing energy.

at 4–5 °C by a Circulator (HAAKE Phoenix, Thermo Electron Corporation). Feed containing drug and stabilizer dissolved in solvent (tetrahydrofuran (THF)) is injected through a 1/16 in. o.d. (i.d. = 0.0127 cm) stainless steel tube inserted into the tee mixer. The feed stream impinges directly into the incoming recirculation stream, and the mixed stream exits from the top leg of the mixer (Figure 2). The sonicator tip is placed ~5 mm above the solvent–antisolvent mixing zone to provide high turbulence and micromixing. Unless noted otherwise, a 3.7 mL solution of feed (25 mg/mL each of drug and stabilizer in THF) is injected via a 20 mL glass syringe driven by a syringe pump into the aqueous phase to give final drug concentration of 1.17 mg/mL.

The nanoparticle dispersion, NP, after injection of all of the organic solvent stream was divided into three batches for the stability analysis. The first batch was stored at 5 °C, and will be referred as NPCT (nanoparticle at cold temperature). The second batch was dialyzed against pure water at 5 °C for a day using a Spectra/Por dialysis membrane with MWCO 6K–8K and thereafter stored at 5 °C, referred as NPCTD (nanoparticle cold temperature dialyzed). The last batch was stored at room temperature without dialysis, referred as NPRT (nanoparticle at room temperature). Dynamic laser light scattering was used to determine the particle size (expressed as the number weighted diameter) with a Nanotracer particle size analyzer (Nanotracer NPA 250) using the microtrac FLEX application software. All measurements were made with a laser diode of 780 nm wavelength at the scattering angle of 180°. The results are listed as D10/D50/D90, which denotes the diameter of the 10th, 50th and 90th percentile of the distribution. The nanoparticle suspensions were gently hand-shaken, but were not filtered, before the size analysis.

#### High Performance Liquid Chromatography (HPLC).

To determine the solubility, 0.25 mg/mL of bulk ITZ and ODA solutions were stirred at room temperature and 5 °C for 3 days. An aliquot of suspension was centrifuged at 15,000 rpm for 10 min, and the supernatant was filtered through 0.22 µm filter for analysis via HPLC. HPLC was performed to determine the drug concentrations. The mobile phase consisting of 0.1% phosphoric acid/acetonitrile (90:

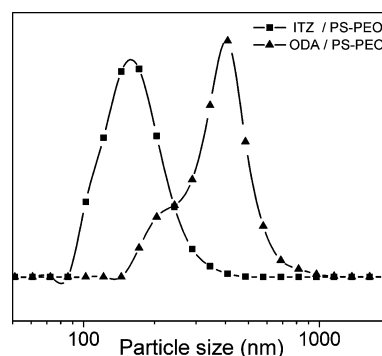


**Figure 3.** Initial particle size distribution of PS-*b*-PEO stabilized nanoparticles of ITZ and ODA. ODA resulted in a larger sized particle of ~352 nm (204/347/479) compared to ITZ particles of size ~140 nm (102/133/185).

10 vol:vol) was used with a Zorbax SB-Aq column at a flow rate of 1.5 mL/min for ITZ, and water/acetonitrile (50:50 vol:vol) was used with an Ace 3 Phenyl column at a flow rate of 1.2 mL/min for ODA. The column was maintained at 40 °C, and the UV detector was set at 210 and 266 nm for ITZ and ODA, respectively.

**Materials.** ITZ was obtained from Neuland Laboratories, India, and ODA was obtained from Merck Co. USA. PS<sub>1k</sub>-*b*-PEO<sub>3k</sub> (1,000 *M*<sub>w</sub> polystyrene-block-3,000 *M*<sub>w</sub> polyethylene oxide) stabilizing polymer was obtained from Goldschmidt AG, Essen, Germany. Poloxamer P407, a block copolymer of polypropylene oxide and polyethylene glycol (PEG-*b*-PPO-*b*-PEG), was obtained from BASF, Germany. Note that polyethylene glycol and polyethylene oxide are identical compounds; their different nomenclature comes from their differing starting monomers. All solvents were used as received.

## Results and Discussion

Nanoparticles of drug compounds ITZ and ODA were formulated with a PS<sub>1k</sub>-*b*-PEO<sub>3k</sub> as the stabilizer. ODA produced a larger initial particle size of ~352 nm compared to ITZ (~145 nm) as shown in Figure 3. The initial particle size depends on the rate of nucleation and subsequent growth on the nuclei. The rate of nucleation, *J*, is given by<sup>19</sup>

$$J \propto \exp \left[ -\frac{16\pi\gamma^3 v^2}{3k_B^3 T^3 (\ln S)^2} \right] \quad (1)$$

where  $\gamma$  is solid–liquid interfacial tension of the solute,  $v$  is molar volume of the solute, and  $S$  is the supersaturation ratio defined as the solute concentration in the mixed aqueous phase after micromixing divided by the solubility of the solute in the mixed aqueous phase. The interfacial tension can be estimated by<sup>20</sup>

$$\gamma_{sw} = 0.414k_B T (N_A/v)^{2/3} \cdot \ln \left( \frac{1}{v \cdot c^\infty} \right) \quad (2)$$

$N_A$  is the Avogadro constant,  $k_B$  is the Boltzmann constant, and  $T$  is the temperature (K). The values of solubility for

(19) Mullin, J. W. *Crystallization*, 3rd ed.; Butterworth Heinemann: Oxford, U.K., 1993; p 176.

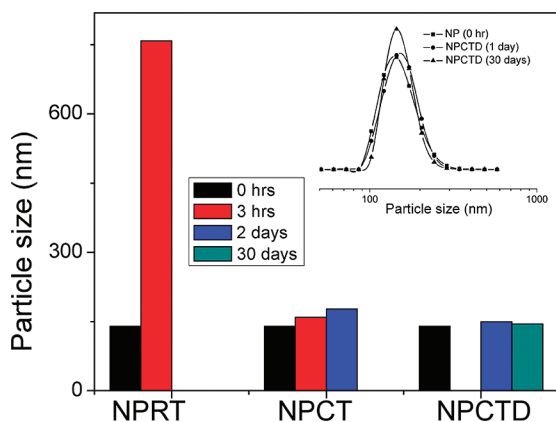
**Table 1.** Bulk Solubility of Drug Compounds in Water–THF Solutions at Different Temperatures and Concentrations of THF in the Aqueous Phase

solute	MW (g/mol)	solubility (mol/m <sup>3</sup> )		
		room temp		cold temp (5 °C)
		4.7 vol % THF	4.7 vol % THF	0% THF
ITZ	705.64	$1.45 \times 10^{-4}$	$1.18 \times 10^{-4}$	$0.28 \times 10^{-4}$
ODA	525.57	$13.0 \times 10^{-4}$	$12.0 \times 10^{-4}$	$5.7 \times 10^{-4}$

**Table 2.** Process and Solute Parameters for the Formulation of Nanoparticles<sup>a</sup>

solute	molar vol, <sup>b</sup> $v$ (m <sup>3</sup> /mol)	supersaturation ratio, $S$	interfacial tension, $\gamma$ (N/m)
ITZ	$5.10 \times 10^{-4}$	$1.41 \times 10^{+4}$	$2.96 \times 10^{-2}$
ODA	$3.75 \times 10^{-4}$	$1.86 \times 10^{+3}$	$3.18 \times 10^{-2}$

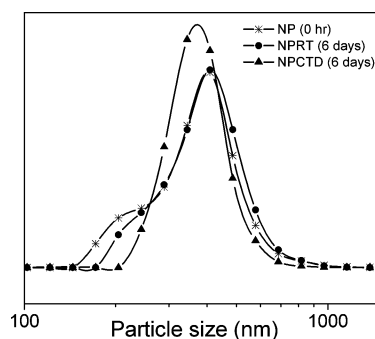
<sup>a</sup> Formulation conditions: temperature = 5 °C, solute concentration in final mixed NP dispersion = 1.17 mg/mL, 4.7 vol % THF present in final suspension. <sup>b</sup> Molar volumes were calculated from the measured solid density of solutes by pycnometer. Solid density: for ITZ, 1.38 g/mL; and ODA, 1.40 g/mL.

**Figure 4.** Dependence of stability of ITZ nanoparticle on different storage conditions. Particles stored at room temperature (NPRT) increased to ~758 nm (653/746/849) in 3 h while the sample stored at 5 °C (NPCT) only increased to ~177 nm (124/167/240) in 2 days. The dialyzed sample (NPCTD) was stable at ~145 nm for over a month. The inset shows the size distribution of dialyzed ITZ particles at 5 °C stabilized by PS-*b*-PEO, (NPCTD).

the two compounds at different conditions were determined via HPLC and are presented in Table 1. Table 2 gives the values of interfacial tension and supersaturation ratio attained by drug molecules under the experimental conditions.

Using eq 1, the rate of nucleation for ITZ was calculated to be ~3 times faster than that of ODA, which correlates well with the latter being ~2.43 times larger in size. The slower the rate of nucleation, the lower will be the number of nuclei formed. This results in a larger particle size after addition of solutes onto the smaller number of nuclei.

**Itraconazole Formulation and Stability.** Figure 4 shows the dependence of nanoparticle size on the storage conditions for PS-*b*-PEO stabilized particles. The initial particle size

**Figure 5.** Stability of ODA particles stabilized by PS-*b*-PEO. Particles stored at room temperature, NPRT, showed a small increment in size to ~370 nm (233/362/498) while the dialyzed sample stored at 5 °C, NPCTD, was stable at ~350 nm (260/338/442).

of ITZ was ~140 nm (102/133/185). Temperature is a critical parameter in determining the stability of ITZ nanoparticle. The increment in size of the undialyzed sample, NPCT, was ~15% in 2 days compared to the 5-fold increase in size at room temperature in 3 h (NPRT). Solvent removal (4.7% by volume of THF present in NPCT) by dialysis further enhances the stability resulting in a stable dispersion over a 30 day period (NPCTD) (Figure 4).

**ODA Formulation and Stability.** Temperature and solvent concentration were not significant variables for the stability of ODA nanoparticles (Figure 5). The dialyzed suspension, NPCTD, was stable with a size ~350 nm after a month of storage at 5 °C.

The reason for the relative instability of ITZ particles compared to the ODA particles can be explained through the Ostwald ripening mechanism<sup>19</sup> (eq 3). The particle solubility  $c(r)$  is governed by particle radius ( $r$ ), molar volume of the solute ( $v$ ), equilibrium solubility ( $c^\infty$ ), and the solid–liquid interfacial tension of the solute ( $\gamma$ );  $R$  is the gas constant.

$$\ln\left(\frac{c(r)}{c^\infty}\right) = \frac{2\gamma v}{RTr} \quad (3)$$

For diffusion-controlled growth kinetics, the growth velocity is given by<sup>17,19</sup>

$$\frac{dr}{dt} \approx \frac{\gamma v^2 D c^\infty}{3RTr^2} \quad (4)$$

where  $D$  is the diffusion coefficient of a solute molecule in solution. Integrating eq 4 gives the time scale for diffusion-controlled growth kinetics as<sup>19</sup>

$$t_d \approx \frac{RTr^3}{\gamma v^2 D c^\infty} \quad (5)$$

Since the solubility varies with temperature and organic solvent concentration, the calculated time scale of ripening for different nanoparticle dispersions was mapped against the bulk solubility in Figure 6. The time scale for Ostwald ripening in eq 5 provides a framework for understanding the parameters that control stability.<sup>17</sup> However, effects such as



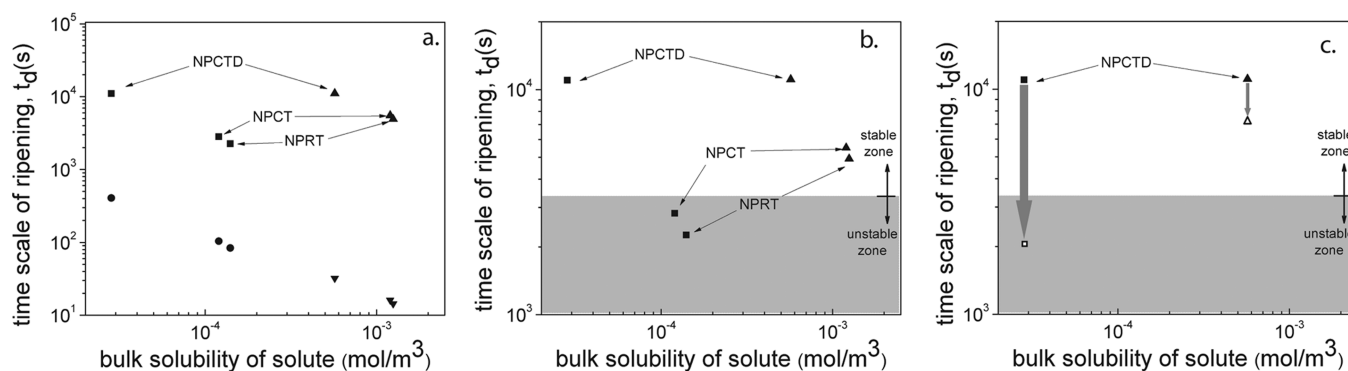


**Figure 6.** Calculated ripening time scale of ITZ and ODA nanoparticles under different process conditions with differing drug solubilities in the aqueous solution: room temperature with 4.7 vol % THF (NPRT), 5 °C with 4.7 vol % THF (NPCT), and 5 °C dialyzed to remove THF (NPCTD). (a) Time scale of ripening for ITZ and ODA nanoparticles with variation in size for the three process conditions: ITZ (150 nm) [■], ODA (350 nm) [▲]; ITZ (50 nm) [●], and ODA (50 nm) [▼]. (b) Experimentally observed boundaries between stable and unstable formulations of ITZ and ODA nanoparticles with PS-*b*-PEO as the stabilizer. Particles in the gray area were unstable within 2 days of storage. (c) Impact of stabilizer on stability. Poloxamer P407 nanoparticles are less stable than PS-*b*-PEO nanoparticles due to the higher effective bulk solubility of drug molecules in the P407 solution. The block arrows show the decrease in ripening time scale, using the effective bulk solubility in 6 mg/mL P407 solution, pulling the dialyzed ITZ particles (NPCTD) into the unstable zone, while dialyzed ODA particles remain stable. The open symbols show the calculated ripening time using the measured drug solubilities from Table 3.

**Table 3.** Solubility (mol/m<sup>3</sup>) of ITZ and ODA Drug Compounds in Water and Poloxamer P407 Solutions<sup>a</sup>

compound	DI water	poloxamer P407–water solution	
		1.2 mg/mL P407 solution	6 mg/mL P407 solution
ITZ	$2.83 \times 10^{-5}$	$4.39 \times 10^{-5}$	$15.6 \times 10^{-5}$
ODA	$5.71 \times 10^{-4}$	$6.28 \times 10^{-4}$	$8.94 \times 10^{-4}$

<sup>a</sup> All data are at 5° C.

the presence of the stabilizing polymer on the process make the calculations qualitative rather than quantitative. Below we show how the scaling suggested by eq 5 guides our understanding of diffusion-controlled particle size changes.

**Factors Controlling Stability.** *Particle Size and Drug Solubility.* Figure 6a demonstrates the effect of size and solubility on the ripening rate, emphasizing the significance of size over solubility. The bulk solubility,  $c^\infty$ , of ODA (NPRT) is  $\sim 9$  times higher than that of ITZ (NPRT), but owing to the smaller molar volume and larger size of the ODA nanoparticles, the time scale of ripening for ODA particles (NPRT) is longer than that for ITZ particles (NPRT), and hence, the ODA nanoparticles are more stable. This effect is predicted by eq 5. For the same storage conditions, hypothetical particles of smaller size (50 nm) of either compound would be unstable with the 50 nm ODA particles being less stable than the ITZ owing to ODA's higher bulk solubility. Based on the experimental observations the boundary between stable and unstable particle formulations is shown. Of course, the boundary for stability is defined for our arbitrary observation window of 30 days.

*Stabilizing Polymer Type.* The analysis above does not take into account the impact of stabilizers on the ripening. Two stabilizing polymers were used to produce nanoparticles: PS-*b*-PEO and PEG-*b*-PPO-*b*-PEG, Pluronic P407. Both poly-

mers have PEG stabilizing blocks. The hydrophobic blocks differ considerably. At the used temperature range of 4–25 °C, the PS block ( $T_g = 95$  °C)<sup>21</sup> exists as a glassy structure compared to the liquid state for PPO ( $T_g = -75$  °C).<sup>22</sup>

ITZ nanoparticles formulated with poloxamer P407 with an initial size of  $\sim 158$  nm were stable only for a few days at 5 °C, even after dialysis. For ODA/P407 particles with an initial size of  $\sim 350$  nm, only the dialyzed sample stored at 5 °C was stable. As water is mixed against THF during formation, the solubilities of PPO and PS blocks decrease by almost the same extent owing to their similar solubility parameters<sup>23</sup> ( $\delta_{PS} = 18.6$  MPa<sup>1/2</sup>;  $\delta_{PPO} = 19.0$  MPa<sup>1/2</sup>). Consequently the attachment energies of these two polymers on the nanoparticle surface should be nearly equal, and we observe that both stabilizers produce similarly sized initial nanoparticles.

However, the nature of the polymer plays an important role in determining the long-term stability of nanoparticles. The stabilizing polymer may influence long-term stability in three ways: (1) differing steric stabilizing efficiencies against aggregation, (2) differing diffusional resistance of the drug through the hydrophobic block encapsulating layer, or (3) increased solubility of the drug in the aqueous phase due to micellization by the block copolymer. The data would

- (20) Mersmann, A. Calculation of interfacial tensions. *J. Cryst. Growth* **1990**, *102*, 841–847.
- (21) Forrest, J. A.; Dalnoki-Veress, K.; Dutcher, J. R. Interface and chain confinement effects on the glass transition temperature of thin polymer films. *Phys. Rev. E* **1997**, *56* (5), 5705.
- (22) Jannasch, P. Preparation and characterisation of aggregating comblike poly(propylene oxide). *Polymer* **2000**, *41* (18), 6701–6707.
- (23) Nagarajan, R.; Barry, M.; Ruckenstein, E. Unusual selectivity in solubilization by block copolymer micelles. *Langmuir* **1986**, *2* (2), 210–215.

suggest the first two mechanisms are not the cause. The modest temperature differences and THF concentrations would not change the solubility or conformation of the stabilizing PEG layer significantly. But since the temperature and solvent conditions make a major change in stability, aggregation due to changes in steric stabilization are unlikely. Also, we do not believe that diffusional resistance through the hydrophobic block layer controls release and, therefore, Ostwald ripening kinetics. Diffusion through glassy polymer matrices is orders of magnitude slower than diffusion through polymers above their  $T_g$ ,<sup>24</sup> i.e. in the liquid state, and consequently, if the PS layer formed a conformal, glassy coating around the nanoparticle core, the slower diffusion through PS would increase the ripening time (eq 5) and would result in greater nanoparticle stability. If the PS layer controlled release, a modest change in temperature between 5 and 18 °C should not appreciably change diffusion through the high glass-transition-temperature PS layer. The particle stability was found to be much more dependent on solvent, temperature, and drug type than on the hydrophobic block type (Figure 6b). Furthermore, since modeling of the Ostwald ripening process for PS-*b*-PEO stabilized  $\beta$ -carotene nanoparticles resulted in agreement of the increase in particle size over a range of solvent concentrations with no adjustable parameters,<sup>17</sup> we believe that the hydrophobic layer does not control release. However, work is ongoing in our group to create encapsulating layers that will control release.

We believe the third mechanism, the increased solubilization of the drug by the block copolymer, is the origin of the different stabilities of the nanoparticles. Equation 5 shows that the rate of ripening depends linearly on the (effective) bulk solubility of the drug,  $c_{\text{eff}}^\infty$ . The solubilities of ITZ and ODA in P407/water solutions were measured and are given in Table 3.

The measured bulk solubility of ITZ in 6 mg/mL P407–water solution at 5 °C was  $\sim 5.5$ -fold higher than that in pure water, and ODA was 1.6-fold higher. The increased solubility in the polymer solution is due to uptake of the drug into the cores of polymer micelles. The higher solubilization of ITZ is due to the better match of solubility parameters of ITZ to the hydrophobic polypropylene oxide (PPO) than of ODA to PPO ( $\delta_{\text{PPO}} = 19.0 \text{ MPa}^{1/2}$ ,  $\delta_{\text{ITZ}}^{25} = 21.6 \text{ MPa}^{1/2}$ ,  $\delta_{\text{ODA}} = 22.05 \text{ MPa}^{1/2}$ , the solubility parameters for ODA were calculated by a group contribution method<sup>6,26</sup>). Therefore, the PPO block can better micellize the ITZ and the effective concentration in bulk solution  $c_{\text{eff}}^\infty$  is higher. This increase in Ostwald ripening rate due to increased effective solubility in micelles has been reported for emulsions

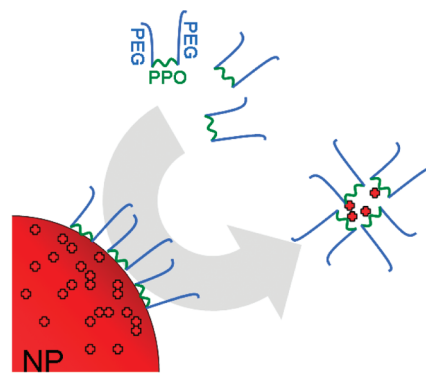


**Figure 7.** Schematic mechanism for increased solubilization of drug molecules at the poloxamer interface. A continuous adsorption of polymer P407 at the nanoparticle surface and desorption (with solubilized drug molecules) leads to particle instability.

previously.<sup>27,28</sup> The solubilization of drug occurs at the nanoparticle surface where the P407 is concentrated by virtue of its adsorption at the drug–water interface. To represent this enhanced concentration at the interface we have chosen a 5-fold enhancement of P407 concentration at the nanoparticle surface. Using the measured solubilities (Table 3) to determine the time scale for ripening (Figure 6c) shows that the ITZ time scale is reduced so that the ITZ particles are predicted to be unstable and the ODA particles are predicted to be stable. These predictions match our experimental observations.

In addition, there appears to be a kinetic aspect to the role of polymers on stability. Both PS and PPO have similar solubility parameters and, therefore, interactions with the drug compounds, as noted above. However, the PS-*b*-PEO stabilized nanoparticles have much greater kinetic stability than the poloxamer stabilized nanoparticles. The difference arises from the high and low glass transition temperatures of the two polymers. After precipitation into nanoparticles and micelles during flash nanoprecipitation, the PS block is frozen ( $T < T_g$  PS). In contrast the PPO block is fluid ( $T > T_g$  PPO). Pena et al.<sup>29</sup> have shown that surfactants or polymers that can adsorb to an interface can desorb with entrained solute and greatly increase the rate of solubilization. The process is schematically shown in Figure 7. This phenomenon is behind the dissolution of grease droplets by dishwashing detergents.<sup>30</sup> A mass transfer model on the dissolution rates of poorly water soluble drugs has previously

(24) Vrentas, J.; Duda, J. A free-volume interpretation of the influence of the glass transition on diffusion in amorphous polymers. *J. Appl. Polym. Sci.* **1978**, 22 (8), 2325–2339.

(25) Constantinides, P. P.; Han, J.; Davis, S. S. Advances in the Use of Tocols as Drug Delivery Vehicles. *Pharm. Res.* **2006**, 23 (2), 243–255.

(26) Barton, A. F. *CRC Handbook of Solubility Parameters and Other Cohesion Parameters*; CRC Press: Boca Raton, 1991; p 739.

(27) Liu, W.; Sun, D.; Li, C.; Liu, Q.; Xu, J. Formation and stability of paraffin oil-in-water nano-emulsions prepared by the emulsion inversion point method. *J. Colloid Interface Sci.* **2006**, 303 (2), 557–563.

(28) Wooster, T. J.; Golding, M.; Sanguansri, P. Impact of Oil Type on Nanoemulsion Formation and Ostwald Ripening Stability. *Langmuir* **2008**, 24 (22), 12758–12765.

(29) Peña, A. A.; Miller, C. A. Solubilization rates of oils in surfactant solutions and their relationship to mass transport in emulsions. *Adv. Colloid Interface Sci.* **2006**, 123–126, 241–257.

(30) Chan, A. F.; Evans, D. F.; Cussler, E. L. Explaining solubilization kinetics. *AIChE J.* **1976**, 22 (6), 1006–1012.

been studied in terms of the uptake and desorption of micelles and diffusion of the drug-loaded micelles.<sup>31</sup> In contrast Bronstein et al.<sup>32</sup> have shown that the kinetically frozen PS-*b*-PEO micelles, once formed, are not subject to dynamic equilibrium and, therefore, would not participate in kinetic solubilization of the drug from the nanoparticle surfaces. So the role of the hydrophobic polymer block has both a thermodynamic role (equilibrium bulk solubility,  $c_{\text{eff}}^{\infty}$ ) and a kinetic aspect governed by the ability of the polymer to dynamically adsorb and desorb from the nanoparticle surface.

## Conclusions

We demonstrate the successful formulation of smaller ITZ nanoparticles than have been previously prepared, and the first successful preparation of ODA nanoparticles. Post

processing conditions including storage at low temperature and removal of residual THF solvent increased nanoparticle stability. Stable ITZ nanoparticles of sub-150 nm were obtained by reducing the solution temperature to 5 °C and removing residual organic solvent by dialysis. The theories of nucleation rates and Ostwald ripening kinetics provide a framework for understanding the physical parameters that control stability: solute solubility, interfacial tension and molar volume. The effect of polymer type on the long-term stability of the nanoparticles was demonstrated by comparing nanoparticles prepared with PS-*b*-PEO and poloxamer P407. The solubility parameter match between ITZ and PPO resulted in higher bulk solubilities and greater instability. The differences in glass transition temperatures (chain mobilities) between PS and PPO showed that glassy or kinetically frozen stabilizing polymers result in more stable nanoparticle formulations.

**Acknowledgment.** The work was supported by Merck Research Laboratories, West Point, US, and the NSF under the NIRT grant to Princeton University.

MP900002T

- 
- (31) Crisp, M. T.; Tucker, C. J.; Rogers, T. L.; Williams, R. O.; Johnston, K. P. Turbidimetric measurement and prediction of dissolution rates of poorly soluble drug nanocrystals. *J. Controlled Release* **2007**, *117* (3), 351–359.
- (32) Bronstein, L. M.; Chernyshov, D. M.; Timofeeva, G. I.; Dubrovina, L. V.; Valetsky, P. M.; Khokhlov, A. R. Polystyrene-block-Poly(ethylene oxide) Micelles in Aqueous Solution. *Langmuir* **1999**, *15* (19), 6195–6200.